Research Article | Vol. 1, No. 2 | 15 Oct 2018 | OSA CONTINUUM 573

OSA CONTINUUM

Infrared metamaterial absorber by using chalcogenide glass material with a cyclic ring-disk structure

ZEFENG XU, RUIJIA XU, JUN SHA, BIN ZHANG, YANLIN TONG, AND YU-SHENG LIN*

State Key Laboratory of Optoelectronic Materials and Technologies, School of Electronics and Information Technology, Sun Yat-Sen University, Guangzhou, 510275, China
**linyoush@mail.sysu.edu.cn*

Abstract: We propose a novel infrared (IR) metamaterial absorber by using chalcogenide glass (ChG) material. The merits of ChG are zero extinction coefficient, excellent IR transparency, high third-order nonlinearity, adjustable refraction index, dispersion, and energy bandgap in the IR wavelength range. Therefore, it is very suitable for metamaterial designs used in widespread applications, such as solar cells, environmental sensors, wearable electronic devices, optoelectronics, and so on. This ChG-based metamaterial absorber is configured with a cyclic ring-disk (CRD) structure. By tailoring the geometrical structures of CRD, the corresponding resonant wavelength and intensity of the reflection spectra could be attenuated and modified. The maximum quality factor (Q-factor) is 625. These unique characteristics of this IR metamaterial absorber with a CRD structure can be used as a tunable IR filter, variable optical attenuator (VOA), and multi-resonance switch. For the applicability of the proposed IR metamaterial absorber, the proposed device is surrounded with different environmental media. The electromagnetic responses indicate that the proposed IR metamaterial absorber can be a high-efficiency environmental sensor with a correlation coefficient of 0.99999.

1. Introduction

Metamaterials are artificial materials composed of periodic or aperiodic structures to have extraordinary electromagnetic characterizations. By properly tailoring the feature size of metamaterial, it can be realized electro-optic devices spanning the wavelength range from microwave, infrared (IR), visible to ultraviolet (UV) caused from the transformation optics [1,2]. In view of metamaterials having unique electromagnetic characterizations that cannot found in nature materials, metamaterials have great potentialities in the development of novel optical devices, such as optical waveguide, filter, switch, nanophotonic, sensor, high-resolution imaging, and so on. Moreover, the development of metamaterials can greatly reduce the volume and weight of conventional optical devices [1]. Recently, there have been reported many literatures for metamaterial-based optoelectronic devices. However, they are almost passive devices and less researches demonstrated active devices by using metamaterials. Although there are abundant results of passive and active devices for the potential applications, such as sensors [3–7], absorbers [8–14], solar cells [15,16], switches [17] and filters [18], their optical performances are not perfect for widespread applications with high portability, applicability, and cost-effectiveness characterizations. Such characteristics of active metamaterial-based devices might minimize limitations of time and space in the uses of energy harvesting, emitter, detector, photovoltaic cell, spectroscopy, sensor and other fields.

In the reported literatures, the uses of materials for metamaterials are including silver (Ag), gold (Au), aluminum (Al), and copper (Cu). Among of these materials, Ag and Au are

#337991 https://doi.org/10.1364/OSAC.1.000573
Journal © 2018 Received 5 Jul 2018; revised 30 Aug 2018; accepted 3 Sep 2018; published 1 Oct 2018

OSA CONTINUUM

the two most often used for metamaterial applications than aluminum (Al) and copper (Cu) due to their relatively small ohmic losses or high conductivity in IR wavelength range. However, Ag material will suffer the degradation in the fabrication process. The critical value of uniform Ag film-thickness is less than 25 nm [19] and the losses of Ag are strongly dependent on the surface roughness [20]. Furthermore, the IR spectra are easily absorbed in Ag and Au materials resulting in low efficiency of electromagnetic response. In this study, we propose a novel IR metamaterial absorber by using chalcogenide glass (ChG) materials. ChG materials are amorphous compound containing the chalcogen elements (S, Se, Te) and exhibit wide IR transparency windows. They are easily synthesized to be a thin-film layer and their compositional flexibility allows the tuning of optical properties making them ideal for optoelectronics applications. The characteristics of ChG materials are zero extinction coefficient, excellent IR transparency, high third-order nonlinearity, adjustable refraction index and energy bandgap in IR wavelength range [21]. Moreover, the feature sizes are less than 2 μm for the ChG with a high nonlinear coefficient, the dispersion of ChG is basically close to zero in near-IR and mid-IR wavelength ranges [22]. These extraordinary characteristics can be utilized micro-electro-mechanical systems (MEMS) technique to modify the electromagnetic response of ChG-based metamaterial absorber with reconfigurable geometrical dimensions. In addition, ChG-based metamaterial absorber can prevent the high absorption comes from traditional metallic materials in IR wavelength range.

Herein, ChG-based metamaterial absorber is composed of an inner disk and an outer ring configuration, which is called the circular ring-disk (CRD) structure on Au/Si substrate. By tailoring the geometrical parameters including refraction index of ChG, CRD radius, gap between inner disk and outer ring, and horizontal relative position of inner disk and outer ring, the resonant frequency and intensity of ChG-based metamaterial absorber can be modified to perform a multi-resonance switch with an ultra-high Q-factor. To further investigate the proposed device can be used in practical applications, ChG-based metamaterial absorber is surrounded with different environmental media. It can be a high-precision refraction index sensor.

2. Designs and methods

Figure 1 shows the schematic drawing of proposed ChG-based metamaterial absorber with CRD structure on Au/Si substrate. The thickness of Au layer is 400 nm. The denotations are diameter of outer ring (*R*), diameter of inner disk (*r*), gap between inner disk and outer ring (*g*), horizontal displacement of outer ring (*d*), refraction index of air (n_0), and refraction index of ChG (n_m), respectively. The line width of ring (*w*) and period of ChG (*p*) are kept at 0.3 μm and 3 μm, respectively. The inner disk is fixed on Au/Si substrate and the outer ring is designed to be suspended and adjustable. The gap between inner disk and outer ring and horizontal displacement of outer ring can be modified by using MEMS-based electrostatic or electrothermal actuation mechanism to realize tunable metamaterial. According to the propagation and attenuation of surface plasmon polaritons (SPPs) on metamaterial absorber, it can generate the collective oscillation of free electrons within metamaterial absorber when the wavevector of SPPs is equal to that of incident electromagnetic wave [23] and then the incident electromagnetic energy will be absorbed by these metamaterial structures. We propose an active tuning approach to control ChG-based metamaterial absorber by using Lumerical Solution’s finite difference time domain (FDTD) based simulations to study the optical properties of device. The propagation direction of incident light is set to be perpendicular to the *x*-*y* plane in the numerical simulations. Periodic boundary conditions are also adopted in the *x* and *y* directions and perfectly matched layer (PML) boundaries conditions are assumed in the *z* direction. The mesh precision is 0.5 nm and the minimum clearance size is 0.1 μm. The reflection (*R*) and transmission (*T*) of lights are calculated by two monitors set on both sides of device. The corresponding absorption (*A*) is defined as $A = 1\text{-}R\text{-}T$. Since transmission is inhibited by the opaque bottom Au layer, and then the absorption can be directly obtained by A = 1-R. It means the high absorption obtained by the low reflection.

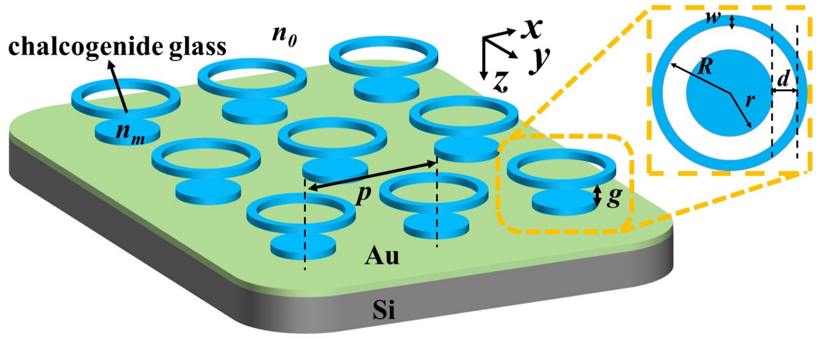

Fig. 1. Schematic drawing of ChG-based metamaterial absorber with CRD structure.

3. Results and discussions

Figure 2 shows the reflection spectra of ChG-based metamaterial absorber with CRD structure by changing the refraction index of ChG (n_m) from 2.0 to 3.4. The geometrical dimensions are kept at R = 1.2 μm, r = 0.8 μm, g = 0, and d = 0.4 μm, respectively. The tuning range of resonance is 0.42 μm from 3.11 μm to 3.53 μm. The trend and bandwidth of resonances are linear and broader by changing the refraction index of ChG. The resonant intensities are increased gradually at the condition of n_m changing from 2 to 2.4 and then decreased gradually at the condition of n_m changing from 2.4 to 3.4. The maximum resonance is under the condition of n_m = 2.4. The corresponding Q-factor is calculated as 567. The electric (E) and magnetic (H) field distributions for the condition of n_m = 2.4 are shown in Fig. 2(b) and 2(c), respectively. It can be seen the most of electromagnetic energy is focused within the ring and disk of CRD structure.

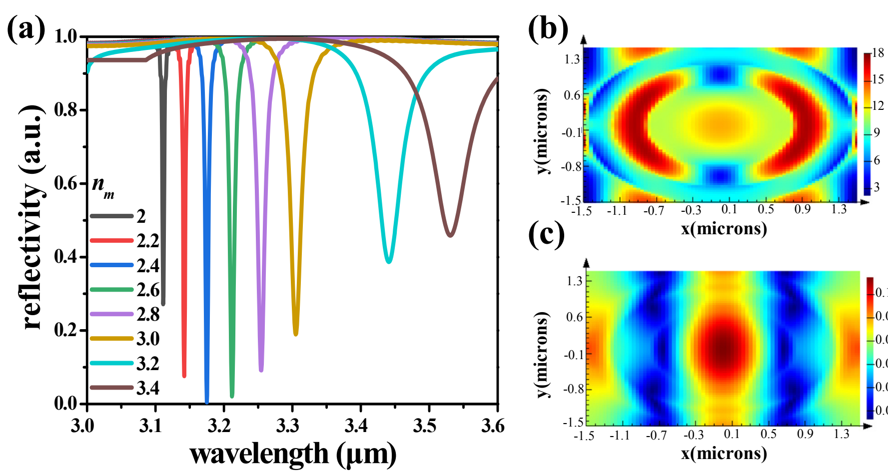

Fig. 2. (a) Reflection spectra of ChG-based metamaterial absorber with CRD structure by changing refraction index of ChG (n_m). The outer ring and inner disk of CRD structure are kept at R = 1.2 μm and r = 0.8 μm on the same plane (g = 0 μm). (b) and (c) are the corresponding E-field and H-field distributions of ChG-based metamaterial absorber with CRD structure at the condition of n_m = 2.4, respectively.

The resonance shifts of ChG-based metamaterial absorber with CRD structure by changing r and R are shown in Fig. 3(a) and 3(b), respectively. In Fig. 3(a), the reflection spectra are red-shifted, while the resonances become strongest by increasing r from 0.6 μm to 1.1 μm. The geometrical parameters are kept at R = 1.2 μm, g = 0, and d = 0.4 μm, respectively. The corresponding Q-factors are calculated in the range of 440 to 567. These values are higher than that reported in literatures [24–26]. In Fig. 3(b), the reflection spectra are almost constant, which variation of resonances is less than 200 nm by increasing R from 0.8 μm to 1.2 μm. The geometrical parameters are kept at r = 0.8 μm, g = 0, and d = 0.4 μm, respectively. The resonant intensity is enhanced by increasing R. The strongest resonance is under the condition of R = 1.2 μm, which is ideal perfect reflection. According to above-mentioned results, it can be concluded that the optimized geometrical parameters of ChG-based metamaterial absorber with CRD structure are n_m = 2.4, r = 0.8 μm, and R = 1.2 μm to exhibit a strongest resonance and an ultra-high Q-factor.

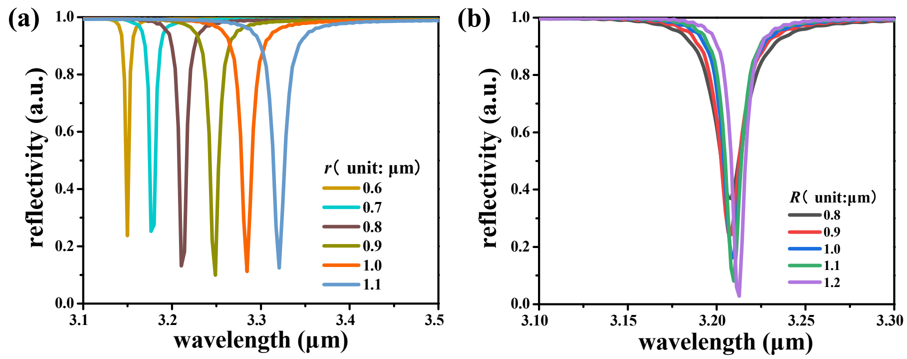

Fig. 3. Reflection spectra of ChG-based metamaterial absorber with CRD structure by changing (a) diameter of inner disk (r) and (b) diameter of outer ring (R), respectively.

Figure 4 shows the reflection spectra of ChG-based metamaterial absorber with CRD structure by changing the gap between inner disk and outer ring (g) from 0 μm to 3 μm. The other geometrical parameters are kept at R = 1.2 μm, r = 0.8 μm, n_m = 2.4, and d = 0.4 μm, respectively. The resonance is blue-shifted by increasing g parameter. The effective tuning range of resonance is between g = 0 μm to 2 μm. According to the theory of gap-mode resonance [27], the Q-factor of device can be enhanced by changing g parameter. The maximum Q-factor is 625 at the condition of g = 1 μm. The corresponding E and H-fields distributions are shown in Fig. 4(b) and 4(c), respectively. The electromagnetic energy is focused on the gap of inner disk and outer ring of CRD structure. The optimized geometrical parameters to earn an ultra-high Q-factor are R = 1.2 μm, r = 0.8 μm, n_m = 2.4, d = 0.4 μm, and g = 1 μm, respectively.

OSA CONTINUUM

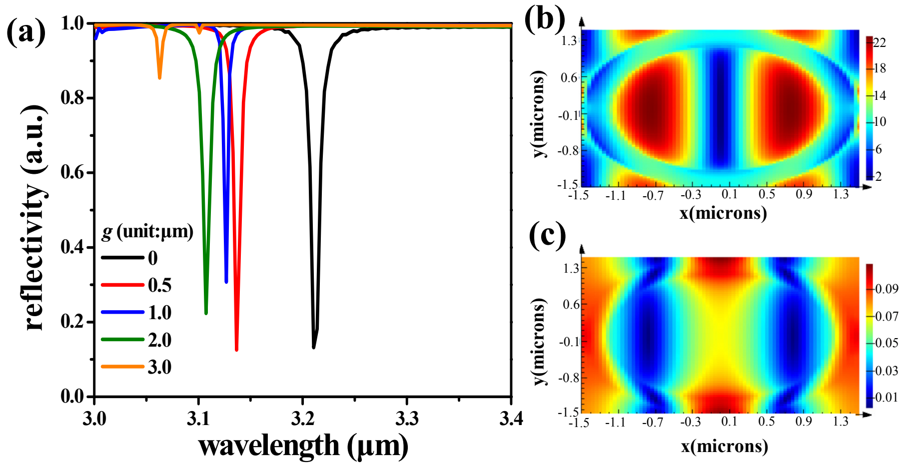

Fig. 4. (a) Reflection spectra of ChG-based metamaterial absorber with CRD structure by changing the gap between inner disk and outer ring (*g*). (b) and (c) are corresponding E-field and H-field distributions under the condition of R = 1.2 μm, r = 0.8 μm, and g = 1 μm, respectively.

To investigate our proposed device to have high flexibility, the influence of horizontal displacement of outer ring (*d*) is compared and discussed to perform multi-resonances switch function. Figure 5 shows the reflection spectra of ChG-based metamaterial absorber with CRD structure by changing *d* parameter from 0.4 μm to 0 μm. The geometrical parameters are kept at R = 1.2 μm, r = 0.8 μm, g = 0 μm, and n_m = 2.4, respectively. There are three resonances at the wavelengths of 3.075 μm, 3.125 μm, and 3.175 μm, respectively. For the condition of d = 0.4 μm, there is a resonance at 3.125 μm wavelength caused from CRD is asymmetrical structure, whose corresponding Q-factor is 479. By shrinking *d* parameter, the resonance will be vanished gradually at 3.125 μm wavelength, while the adjacent both resonances (at 3.075 μm and 3.175 μm wavelengths) will be generated and sharped gradually. In Fig. 5(a)–5(c), there is almost only one resonance at 3.125 μm wavelength that resonant intensity is decreased gradually. The maximum Q-factor is calculated as 567. By continuously changing *d* parameter equals the values of 0.25 μm, 0.20 μm, and 0.15 μm, there has three resonances at 3.075 μm, 3.125 μm, and 3.175 μm wavelengths as shown in Fig. 5(d)–5(f). While the outer ring of CRD is close to the central disk with d = 0.10 μm, d = 0.05 μm, and then touches each other (d = 0 μm), the central resonance (3.125 μm wavelength) is gradually vanished and the adjacent both resonances become stronger as shown in Fig. 5(g)–5(i). The maximum Q-factors are 439 and 489 for resonances at 3.075 μm and 3.175 μm wavelengths, respectively. These resonances exhibit high-performance attenuation and switch functions that can be used for variable optical attenuator (VOA) and multi-resonance switch applications. The corresponding E-field and H-field distributions of ChG-based metamaterial absorber with CRD structure under the conditions of d = 0.40 μm, d = 0.20 μm, and d = 0 μm are shown in Fig. 6(a)–6(c), respectively. That can be explained by the distributions of electromagnetic energy within the gap between inner disk and outer ring of CRD, which is decreased and possesses single, triple and dual resonances for the conditions of d = 0.40 μm, d = 0.20 μm, and d = 0 μm, respectively. Therefore, the proposed ChG-based metamaterial absorber with CRD structure exhibits multi-resonance switch function by changing the horizontal displacement of outer ring.

OSA CONTINUUM

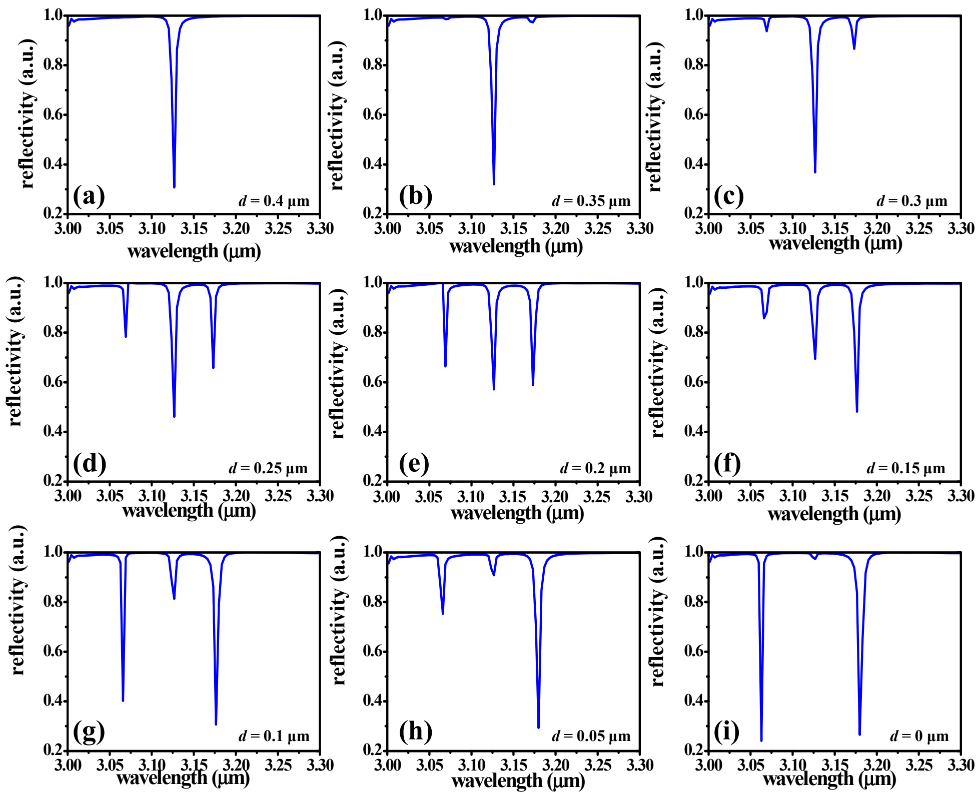

Fig. 5. Reflection spectra of ChG-based metamaterial absorber with CRD structure by changing horizontal displacement of outer ring (d) at (a) d = 0.4 μm, (b) d = 0.35 μm, (c) d = 0.30 μm, (d) d = 0.25 μm, (e) d = 0.20 μm, (f) d = 0.15 μm, (g) d = 0.10 μm, (h) d = 0.05 μm, (i) d = 0 μm, respectively.

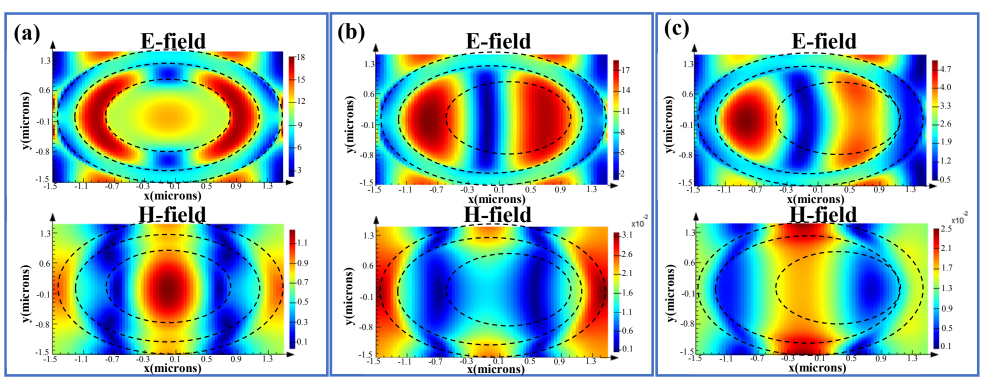

Fig. 6. E-field and H-field distributions of ChG-based metamaterial absorber with CRD structure under the conditions of (a) d = 0.4 μm, (b) d = 0.2 μm, and (c) d = 0 μm, respectively.

To further prove the applicability of proposed ChG-based metamaterial absorber with CRD structure, the proposed device is designed to be surrounded with different environmental media to demonstrate for the high-efficiency environmental sensor application. Figure 7 shows the reflection spectra of ChG-based metamaterial absorber with CRD structure by changing ambient reflection index (n_0) from 1.0 to 1.9. The geometrical parameters are kept at R = 1.2 μm, r = 0.8 μm, n_m = 2.4, g = 0 μm, d = 0.4 μm, respectively.

The resonant intensity is decreased gradually by increasing n_0. The Q-factors are calculated in the range of 265 to 370. The corresponding relationship of resonance and n_0 is summarized in Fig. 7(b). The trend is linear, whose correlation coefficient is 0.99999. This value is better than those reported in literatures [23–26]. Such design of ChG-based metamaterial absorber with CRD structure can be used as a high-efficiency environmental sensor.

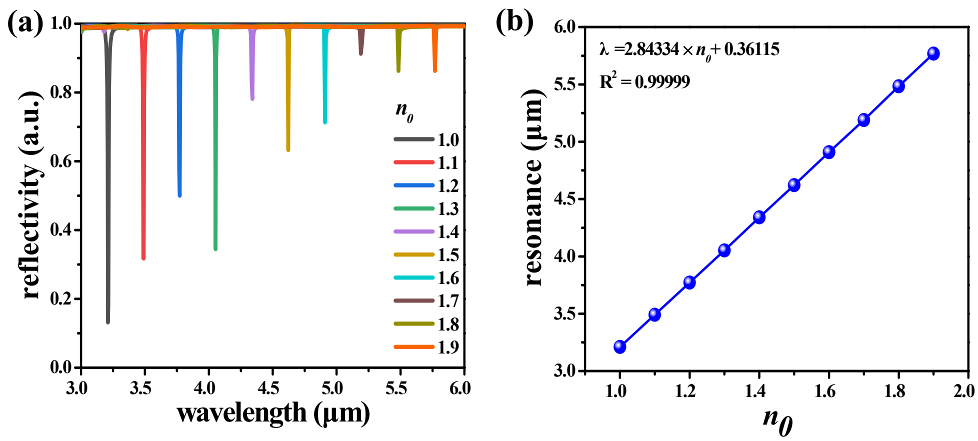

Fig. 7. (a) Reflection spectra of ChG-based metamaterial absorber with CRD structure by changing ambient reflection index (n_0). (b) The relationship of resonance and reflection index (n_0).

4. Conclusion

In conclusion, we present a novel IR metamaterial absorber composed of ChG material with CRD structure. The device possesses tunabilities of resonance and reflection intensity. By tailoring the geometrical dimensions, the reflection spectra of ChG-based metamaterial absorber with CRD structure can be attenuated and modified for the uses of tunable filter, VOA, and multi-resonance switch. The optimized geometrical parameters are R = 1.2 μm, r = 0.8 μm, n_m = 2.4. The reflection spectra can be tuned and switched by single, dual, and triple resonances by changing the distance of inner disk and outer ring of CRD structure. The maximum Q-factors are 625 and 567 for the applications of IR filter and multi-resonance switch, respectively. To further demonstrate the proposed device can be used as high-efficiency environmental sensor, device is designed to be surrounded with different environmental media with different ambient refraction indexes from 1.0 to 1.9. The Q-factors are in the range of 265 to 370 with a linear relationship, whose corresponding correlation coefficient is 0.99999. Such proposed ChG-based metamaterial absorber with CRD structure exhibits unique characteristics for high-performance optoelectronic devices, which will open an avenue to widespread applications, such as filter, VOA, multi-resonance switch, thermal emitter, photodetector, environmental sensor, and so on.

Funding

Research grants of 100 Talents Program of Sun Yat-Sen University (76120-18831103); Science and Technology Planning Project of Guangdong Province (2017B010123005).

Acknowledgment

The authors acknowledge the State Key Laboratory of Optoelectronic Materials and Technologies of Sun Yat-Sen University for the use of simulation codes.

OSA CONTINUUM

References

1. C. M. Soukoulis and M. Wegener, "Past achievements and future challenges in the development of three-dimensional photonic metamaterials," Nat. Photonics **5**(9), 523–530 (2011).
2. Y. S. Lin, F. Ma, and C. Lee, "Three-dimensional movable metamaterial using electric split-ring resonators," Opt. Lett. **38**(16), 3126–3128 (2013).
3. N. Fang, H. Lee, C. Sun, and X. Zhang, "Sub-diffraction-limited optical imaging with a silver superlens," Science **308**(5721), 534–537 (2005).
4. N. Liu, M. Mesch, T. Weiss, M. Hentschel, and H. Giessen, "Infrared perfect absorber and its application as plasmonic sensor," Nano Lett. **10**(7), 2342–2348 (2010).
5. Y. Chuo, D. Hohertz, C. Landrock, B. Omrane, K. L. Kavanagh, and B. Kaminska, "Large-area low-cost flexible plastic nanohole arrays for integrated bio-chemical sensing," IEEE Sens. J. **13**(10), 3982–3990 (2013).
6. N. Li, A. Tittl, S. Yue, H. Giessen, C. Song, B. Ding, and N. Liu, "DNA-assembled bimetallic plasmonic nanosensors," Light Sci. Appl. **3**(12), e226 (2014).
7. Y. Lochbaum, Y. Fedoryshyn, A. Dorodnyy, U. Koch, C. Hafner, and J. Leuthold, "On-chip narrowband thermal emitter for mid-IR optical gas sensing," ACS Photonics **4**(6), 1371–1380 (2017).
8. T. A. Schaedler, C. J. Ro, A. E. Sorensen, Z. Eckel, S. S. Yang, W. B. Carter, and A. J. Jacobsen, "Designing metallic micro lattices for energy absorber applications," Adv. Eng. Mater. **16**(3), 276–283 (2014).
9. K. Chen, R. Adato, and H. Altug, "Dual-band perfect absorber for multispectral plasmon-enhanced infrared spectroscopy," ACS Nano **6**(9), 7998–8006 (2012).
10. S. Xiao, T. Wang, Y. Liu, C. Xu, X. Han, and X. Yan, "Tunable light trapping and absorption enhancement with graphene ring arrays," Phys. Chem. Chem. Phys. **18**(38), 26661–26669 (2016).
11. T. Maier and H. Brückl, "Wavelength-tunable microbolometers with metamaterial absorbers," Opt. Lett. **34**(19), 3012–3014 (2009).
12. J. H. Lee, L. Wang, M. C. Boyce, and E. L. Thomas, "Periodic bicontinuous composites for high specific energy absorption," Nano Lett. **12**(8), 4392–4396 (2012).
13. G. Evans, M. Y. He, V. S. Deshpande, J. W. Hutchinson, A. J. Jacobsen, and W. B. Carter, "Concepts for enhanced energy absorption using hollow micro-lattices," Int. J. Impact Eng. **37**(9), 947–959 (2010).
14. Y. Zhang, T. Li, Q. Chen, H. Zhang, J. F. O'Hara, E. Abele, A. J. Taylor, H. T. Chen, and A. K. Azad, "Independently tunable dual-band perfect absorber based on graphene at mid-infrared frequencies," Sci. Rep. **5**(1), 18463 (2016).
15. G. Dolling, M. Wegener, C. M. Soukoulis, and S. Linden, "Negative-index metamaterial at 780 nm wavelength," Opt. Lett. **32**(1), 53–55 (2007).
16. J. You, Z. Hong, Y. M. Yang, Q. Chen, M. Cai, T. B. Song, C. C. Chen, S. Lu, Y. Liu, H. Zhou, and Y. Yang, "Low-temperature solution-processed perovskite solar cells with high efficiency and flexibility," ACS Nano **8**(2), 1674–1680 (2014).
17. J. J. Talghader, A. S. Gawarikar, and R. P. Shea, "Spectral selectivity in infrared thermal detection," Light Sci. Appl. **1**(8), e24 (2012).
18. F. Guo, T. Sun, F. Cao, Q. Liu, and Z. Ren, "Metallic nanostructures for light trapping in energy-harvesting devices," Light Sci. Appl. **3**(4), e161 (2014).
19. T. W. H. Oates and A. Mücklich, "Evolution of plasmon resonances during plasma deposition of silver nanoparticles," Nanotechnology **16**(11), 2606–2611 (2005).
20. V. P. Drachev, U. K. Chettiar, A. V. Kildishev, H. K. Yuan, W. Cai, and V. M. Shalaev, "The Ag dielectric function in plasmonic metamaterials," Opt. Express **16**(2), 1186–1195 (2008).
21. Y. Yang, Z. Y. Yang, P. Lucas, Y. W. Wang, Z. J. Yang, A. P. Yang, B. Zhang, and H. Z. Tao, "Composition dependence of physical and optical properties in Ge-As-S chalcogenide glasses," J. Non-Cryst. Solids **440**, 38–42 (2016).
22. J. Gao, F. Yu, T. W. Ge, and Z. Y. Wang, "Dispersion study of chalcogenide glass for mid-IR supercontinuum generation," Infrared Laser Eng. **43**(10), 3368–3372 (2014).
23. Y. S. Lin and W. Chen, "A large-area, wide-incident-angle, and polarization-independent plasmonic color filter for glucose sensing," Opt. Mater. **75**, 739–743 (2018).
24. W. X. Lim and R. Singh, "Universal behaviour of high-Q Fano resonances in metamaterials: terahertz to near-infrared regime," Nano Converg. **5**(1), 5 (2018).
25. P. Gu, L. Qian, Z. D. Yan, W. Y. Wu, Z. Chen, and Z. L. Wang, "Fabrication and infrared-transmission properties of a free-standing monolayer of hexagonal-close-packed dielectric microspheres," Opt. Commun. **419**, 103 (2018).
26. X. Wang, Q. Liao, H. Li, S. Bai, Y. Wu, X. Lu, H. Hu, Q. Shi, and H. Fu, "Near-Infrared Lasing from Small-Molecule Organic Hemispheres," J. Am. Chem. Soc. **137**(29), 9289–9295 (2015).
27. G. Dayal, A. Solanki, X. Y. Chin, T. C. Sum, C. Soci, and R. J. Singh, "High-Q plasmonic infrared absorber for sensing of molecular resonances in hybrid lead halide perovskites," J. Appl. Phys. **122**(7), 073101 (2017).